cmgh
CELLULAR AND MOLECULAR GASTROENTEROLOGY AND HEPATOLOGY

ORIGINAL RESEARCH

Enteric Neuron Imbalance and Proximal Dysmotility in Ganglionated Intestine of the *Sox10*$^{Dom/+}$ Hirschsprung Mouse Model

Melissa A. Musser,[1] Hernan Correa,[2] and E. Michelle Southard-Smith[1]

[1]Division of Genetic Medicine, Department of Medicine, and [2]Department of Pathology, Microbiology and Immunology, Vanderbilt University Medical Center, Nashville, Tennessee

SUMMARY

The *Sox10*$^{Dom/+}$ Hirschsprung disease model exhibits imbalance of neuron subtypes throughout the intestine. These alterations suggest a novel role for *Sox10* in neuron specification and, in light of negligible inflammation, likely contribute to deficits in gastric emptying and small intestine motility.

BACKGROUND & AIMS: In Hirschsprung disease (HSCR), neural crest-derived progenitors (NCPs) fail to completely colonize the intestine so that the enteric nervous system is absent from distal bowel. Despite removal of the aganglionic region, many HSCR patients suffer from residual intestinal dysmotility. To test the hypothesis that inappropriate lineage segregation of NCPs in proximal ganglionated regions of the bowel could contribute to such postoperative disease, we investigated neural crest (NC)-derived lineages and motility in ganglionated, postnatal intestine of the *Sox10*$^{Dom/+}$ HSCR mouse model.

METHODS: Cre-mediated fate-mapping was applied to evaluate relative proportions of NC-derived cell types. Motility assays were performed to assess gastric emptying and small intestine motility while colonic inflammation was assessed by histopathology for *Sox10*$^{Dom/+}$ mutants relative to wild-type controls.

RESULTS: *Sox10*$^{Dom/+}$ mice showed regional alterations in neuron and glia proportions as well as calretinin+ and neuronal nitric oxide synthase (nNOS)+ neuronal subtypes. In the colon, imbalance of enteric NC derivatives correlated with the extent of aganglionosis. All *Sox10*$^{Dom/+}$ mice exhibited reduced small intestinal transit at 4 weeks of age; at 6 weeks of age, *Sox10*$^{Dom/+}$ males had increased gastric emptying rates. *Sox10*$^{Dom/+}$ mice surviving to 6 weeks of age had little or no colonic inflammation when compared with wild-type littermates, suggesting that these changes in gastrointestinal motility are neurally mediated.

CONCLUSIONS: The *Sox10*^{Dom} mutation disrupts the balance of NC-derived lineages and affects gastrointestinal motility in the proximal, ganglionated intestine of adult animals. This is the first report identifying alterations in enteric neuronal classes in *Sox10*$^{Dom/+}$ mutants, which suggests a previously unrecognized role for Sox10 in neuronal subtype specification. *(Cell Mol Gastroenterol Hepatol 2015;1:87–101; http://dx.doi.org/10.1016/j.jcmgh.2014.08.002)*

Keywords: Aganglionosis; Enteric Nervous System; Neural Crest.

The enteric nervous system (ENS) regulates multiple gastrointestinal (GI) functions, including motility, secretion, and inflammatory processes.[1] The ENS originates from neural crest-derived progenitors (NCPs) that migrate from the neural tube to colonize the entire intestine.[1] The normal function of the ENS relies upon complete colonization of the bowel as well as appropriate lineage segregation of NCPs to generate a balanced repertoire of distinct neuron classes and glial cell proportions.

In Hirschsprung disease (HSCR), migrating NCPs fail to populate the distal intestine, leading to a variable length of aganglionic bowel.[2] Mutations in *RET*, *EDNRB*, *EDN3*, or *SOX10* cause HSCR in patients, although other genetic variants influence disease penetrance and the extent of aganglionosis.[2–6] Despite surgical resection of the aganglionic segment, many HSCR patients suffer from residual chronic constipation (5% to 33% of patients) and decreased bowel function.[7] In addition, a substantial number of patients suffer from Hirschsprung associated-enterocolitis.[8] Differences in surgical procedures and recovery explain some adverse outcomes, yet many patients suffer from residual symptoms where no iatrogenic cause is found. An understanding of the processes that contribute to residual symptoms in HSCR patients would serve to better predict which patients will suffer from HSCR-related sequelae and to guide treatment options.

Prior evidence from mouse models with mutations that affect the ENS yet exhibit no overt aganglionosis suggests that deficits in enteric NCP lineage segregation contribute to GI dysmotility.[9] Chronic GI dysfunction in HSCR patients after surgery suggests that HSCR susceptibility genes (eg, *SOX10*) not only contribute to aganglionosis but may also affect ganglionated regions of the bowel. It has been suggested that *Sox10* affects multipotency of neural crest (NC)-derived cells and neuronal and glial specification. However, these

Abbreviations used in this paper: **BAC, bacterial artificial chromosome; ENS, enteric nervous system; GI, gastrointestinal; HSCR, Hirschsprung disease; IHC, immunohistochemistry; NC, neural crest; NCP, neural crest-derived progenitor; nNOS, neuronal nitric oxide synthase; P, postnatal; PBS, phosphate-buffered saline; PCR, polymerase chain reaction.**

2352-345X
http://dx.doi.org/10.1016/j.jcmgh.2014.08.002

implications are derived from in vitro experiments or from other NC-derived structures such as dorsal root ganglia.[10–12] Although *Sox10* is essential for enteric NCP migration and colonization of the bowel, studies to elucidate the role of *Sox10* in NCP fate specification in the ENS in vivo have not been undertaken. Given established roles for *Sox10* outside the ENS and the presence of residual symptoms in HSCR patients, we hypothesized that perturbations in *Sox10* disrupt NCP lineage segregation and alter the function of ganglionated bowel in the $Sox10^{Dom/+}$ HSCR mouse model. To test this hypothesis, we fate-mapped NCPs using a Cre-LoxP system. Fate-mapping and immunohistochemical labeling of cell types in the myenteric plexus revealed that the normal complement of NC-derived lineages is disrupted in the enteric ganglia of $Sox10^{Dom/+}$ mutants. These changes are region specific, and disturbances in specific cell types in the colon correlate with extent of aganglionosis. Alterations seen in neuronal subtype proportions in $Sox10^{Dom/+}$ animals suggest a novel role for Sox10 in neuronal class specification.

Because changes in neuron ratios within enteric ganglia can alter GI motility, we investigated the potential for aberrant intestinal transit in the proximal small intestine of this HSCR model. GI motility assays exposed alterations in gastric emptying and small intestine transit that were age and sex dependent. Our results show that the $Sox10^{Dom}$ HSCR mutation alters NC lineage segregation and GI motility despite the presence and normal density of ENS ganglia in the proximal small intestine. Such changes could partially explain adverse outcomes in surgically treated HSCR patients and help clinicians better identify and treat patients at high risk for experiencing postsurgical GI dysfunction.

Materials and Methods

Animals

$Sox10^{Dom/+}$ and homozygous *B6.Cg-Gt(ROSA)-26Sor*$^{tm9(CAG\text{-}tdTomato/Hze/J}$, hereafter $R26R^{tdTom}$, were maintained on a C57BL/6J background. A *Sox10*-Cre bacterial artificial chromosome (BAC) construct was generated from the regulatory elements of *Sox10* within a well-characterized *Sox10* BAC[13] to obtain high levels of Cre in NC derivatives. The construct includes a nuclear localized Cre sequence connected to a human growth hormone mRNA stabilization sequence.[14,15] LoxP sites in the BAC flanking arms were removed as described by Boyle et al (2008) prior to microinjection of the BAC into fertilized mouse eggs by standard procedures.[16] The resulting $Tg^{(Sox10\text{-}CrehGH)1Sout}$ line, hereafter *Sox10-Cre*, was made congenic on the C3HeB/FeJ background. Transgene-driven reporter expression mirrors known *Sox10* expression in NC-derived lineages (Rosebrock J, Buehler DP, DeKeyser JL, et al., in preparation). Experimental animals for NC-derived lineage quantification were from crosses between $Sox10^{Dom/+}$; *Sox10*-Cre or $Sox10^{Dom/+}$; *Sox10*-Cre/Cre mice to $R26R^{tdTom}$ mice. $Sox10^{Dom/+}$ mice were identified by the presence of white feet and belly spotting as well as discernible hypoganglionosis and/or aganglionosis revealed by the absence of tdTomato fluorescent ganglia in the distal intestine. The $Sox10^{Dom/+}$ recapitulates HSCR in humans with animals exhibiting varying lengths of aganglionosis within the bowel despite harboring the same HSCR-causing mutation. The presence of the *Sox10*-Cre transgene was verified by polymerase chain reaction (PCR) genotyping with primers specific for fragment amplification of the Sp6 arm (Forward: Reverse: GGCACTTTCATGTTATCTGAGG), T7 arm (Forward: AAGAG CAAGCCTTGGAACTG; Reverse: TCGAGCTTGACATTGT AGGAC), and Cre-Recombinase (Forward: GCGGCATG GTGCAAGTTGAAT; Reverse: CGTTCACCGGCATCAACGTTT). Thermocycler conditions for all primers sets listed were as follows: 94°C for 5 minutes [(94°C for 30 seconds, 55°C for 30 seconds, 0.5-second ramp up to 72°C, 72°C for 30 seconds, 0.5-second ramp up to 94°C) 35 times], 72°C for 10 minutes, 4°C indefinitely. The Institutional Animal Care and Use Committee at Vanderbilt University approved all experimental protocols.

Immunohistochemistry

Regions of the duodenum, ileum, and midcolon were collected from postnatal (P) 15–19 day $Sox10^{Dom/+}$ and $Sox10^{+/+}$ littermates. Laminar muscle preparations containing myenteric plexus were isolated and subjected to immunohistochemical (IHC) analysis using the reagents described in Tables 1 and 2.[17] After incubation in primary antibodies, all tissues were rinsed in 1X phosphate-buffered saline (PBS)/0.1%Triton X-100 solution followed by incubation in secondary antibody dilution in block for 1 to 1.5 hours at room temperature. Rinses and incubation in a second secondary antibody dilution was repeated as previously described for double labeling. After secondary antibody incubation, tissues were rinsed in 1X PBS/0.1%Triton X-100 followed by rinses in 1X PBS. Tissue samples were stored in the dark in 1X PBS at 4°C before being mounted onto slides with Aqua-Poly/Mount mounting medium

Table 1. Primary Antibodies Used in Immunohistochemical Analysis

Primary antibody antigen	Host	Supplier	Catalog	Dilution	Tissue fix times
HuC/D	Human	Gift of V. Lennon	NA	1:10,000	20–25 min at RT or O/N at 4°C
FoxD3	Rabbit (polyclonal)	Gift of T. Labosky	NA	1:400	O/N at 4°C
Calretinin	Goat (polyclonal)	Millipore	AB1550	1:2500	20–25 min at RT
NOS1 (K-20)	Rabbit (polyclonal)	Santa Cruz Biotechnology	sc-1025	1:600	O/N at 4°C
s100A1	Sheep (polyclonal)	QED Biosciences	56201	1:3000	O/N at 4°C

Abbreviations: NA, not applicable; O/N, overnight; RT, room temperature.

Table 2. Secondary Antibodies Used in Immunohistochemical Analysis

Secondary antibody detection and type	Supplier	Catalog no.	Dilution[a]
Alexa488 donkey anti-rabbit IgG (H+L)	Jackson ImmunoResearch	711-545-152	1:400
Alexa488 donkey anti-sheep IgG (H+L)	Jackson ImmunoResearch	713-545-147	1:400
Alexa647 donkey anti-rabbit IgG (H+L)	Jackson ImmunoResearch	711-605-152	1:200
DyLight649 donkey anti-human IgG (H+L)	Jackson ImmunoResearch	709-495-149	1:200
Cy2 donkey anti-goat	Jackson ImmunoResearch	705-225-147	1:600

[a]All secondary antibody dilutions listed are based on an initial 1:1 dilution in glycerol.

(Polysciences, Warrington, PA). Z-stack images of samples were captured on a Zeiss LSM 510 confocal microscope (20× objective magnification with 1.5 software zoom; Carl Zeiss, Thornwood, NY) to quantify NC derivatives within the ganglia and primary connectives of the myenteric plexus. Image brightness and contrast were adjusted in Adobe Photoshop (Adobe Systems, San Jose, CA) to aid in cell quantification. We quantified n = 5–6 samples per genotype for all duodenum and ileum NC lineage analyses and n = 5–6 $Sox10^{+/+}$ and n = 10–11 for $Sox10^{Dom/+}$ samples for colon NC lineage analyses.

Gastrointestinal Transit Assays

To determine gastric emptying and small intestine transit rates, 4-week-old (27–30 days) or 6-week-old (42–48 days) mice were gavaged with a rhodamine dextran fluorescence containing meal. Fifteen minutes after gavage, the stomach and 10 equal segments of small intestine were collected and homogenized separately. The fluorescence signal from the stomach and each intestinal segment was read on a Molecular Devices/LJL Analyst HT (Molecular Devices, Union City, CA). Gastric emptying percent was determined by calculating the proportion of fluorescence that had left the stomach to total recovered fluorescence. A small intestine transit score was assigned by determining the geometric mean of fluorescence within the 10 equal small intestine segments. Miller et al[18] originally described and validated this method in rats, and recent studies have used these assays in mice.[19–21] To depict small intestine transit rates, the average percentage contribution of each individual intestine segment to the motility score was calculated. A heat map was generated using MATLAB (Mathworks, Natick, MA), where the intestine segment numbers contributing the most to the small intestine transit score (higher fluorescent intensity) are shown in darker red and those contributing little or none to the score (lower fluorescent intensity) in lighter red. Color intensity in between segment number hashes was interpolated to create each heat map (n = 6–8 mice per genotype, sex, and age).

Inflammation

Transverse sections (5 μM) of entire colon from 6 week or older $Sox10^{Dom/+}$ and $Sox10^{+/+}$ littermates were stained with H&E. An expert pathologist blinded to genotype scored the sample inflammation based on a previously developed scoring system using Hirschsprung mouse models.[22] Specifically, a final score of 0–7 was assigned by assessing the severity of inflammation (0–3, with 0 = no inflammation or rare neutrophils; 1 = mild inflammatory infiltrates with no necrosis, 2 = moderate to marked inflammatory infiltrates and mucosal necrosis, and 3 = transmural necrosis) and depth of inflammation (0–4, with 0 = none, 1 = mucosa, 2 = submucosa, 3 = muscularis propia; 4 = subserosa/serosa).[22] In this analysis, n = 6–9 mice per genotype and per sex.

Statistics

For NC lineage quantification, five duodenal, three ileal, and two colonic images were manually counted for each animal. For $Sox10^{Dom/+}$ mice with hypoganglionosis in the midcolon, additional images were quantified so that a comparable number of neurons were counted between $Sox10^{+/+}$ and $Sox10^{Dom/+}$ mice. We tested for differences in cell type proportions, gastric emptying rates, small intestine transit rates, and inflammation scores using a Student t test assuming unequal variance (Welch t test). Analysis of variance (F test) was used to test for statistical significance of slope and to determine the coefficients of determination (r^2). Statistical analysis was performed using JMP software (version 10; SAS Institute, Cary, NC). Variance is reported as ± the standard error of the mean (SEM). All study authors had access to study data, and all authors reviewed and approved the manuscript.

Results

Fate-Mapping Enteric NC Derivatives with a Sox10-Cre BAC Transgene System

Studies to assess alterations in enteric cell types in vivo have largely focused on comparing total numbers of neurons and glia, although a few studies have assessed neuronal subtypes.[20,23] While informative, IHC analysis alone may not comprehensively identify all NC derivatives in the ENS and may miss alterations in patterning and distribution of enteric ganglia depending on the marker used. Because *Sox10* is ubiquitously expressed in NC cells emerging from the neural tube, the use of *Sox10* regulatory regions linked to a Cre driver enables extensive labeling of NC derivatives (Rosebrock J, Buehler DP, DeKeyser JL, et al., in preparation).[24,25] To visualize NC derivatives within enteric ganglia, we combined a *Sox10*-Cre BAC transgene with a Cre-dependent $R26R^{tdTom}$ reporter in crosses with $Sox10^{Dom/+}$ mice. Analysis of $Sox10^{Dom/+}$ mutants on a mixed background in these crosses is advantageous because this model recapitulates the variable penetrance and severity of

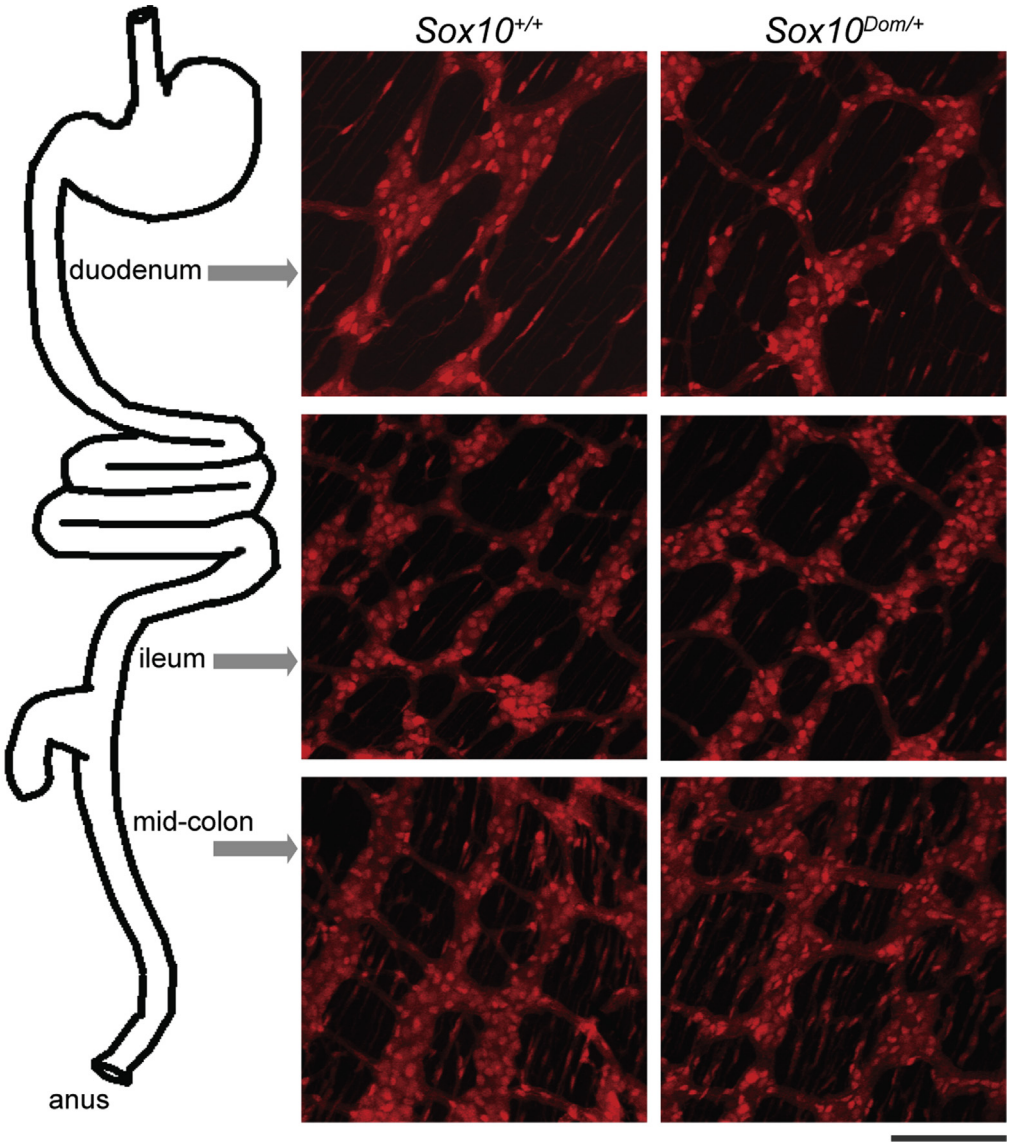

Figure 1. The *Sox10*-Cre transgene system enables visualization of enteric NC derivatives and ENS patterning. Images of P16 *Sox10*$^{+/+}$ and *Sox10*$^{Dom/+}$ mouse duodenum, ileum, and colon are shown. NC derivatives are labeled by activation of the *R26R*^{dTOM} reporter after *Sox10*-Cre transgene expression. *Scale bar* = 100 μm. *Sox10*$^{+/+}$ and *Sox10*$^{Dom/+}$ mice have comparable ENS patterning and overall numbers of NC derivatives in the duodenum $P = .86$ and in the ileum $P = .55$ (n = 5 per genotype).

aganglionosis seen in human HSCR patients.[4,26] In the resulting progeny, the cytoplasmic reporter tdTomato, which is concentrated in the cell soma and labels cellular processes, reveals ganglia structure, density, and connectives of cells in which Cre is expressed. We collected laminar gut muscle preparations in pups between postnatal (P) days 15 and 19, before the majority of these animals succumb to megacolon at weaning. We observed similar myenteric ganglia density, spacing between ganglia, and overall architecture of ganglia in the duodenum, ileum, and ganglionated regions of the colon in both *Sox10*$^{+/+}$ and *Sox10*$^{Dom/+}$ pups (Figure 1). Although comparable ganglia patterning and density were seen, the possibility remained that total numbers of myenteric NCPs might differ between *Sox10*$^{+/+}$ and *Sox10*$^{Dom/+}$ animals and could lead to altered GI function. We compared the total numbers of enteric NC-derived cells between *Sox10*$^{+/+}$ and *Sox10*$^{Dom/+}$ pups. This analysis revealed similar total numbers of NC-derived cells between *Sox10*$^{+/+}$ and *Sox10*$^{Dom/+}$ mice in both duodenum ($P = .86$) and ileum ($P = .55$) (n = 5 per genotype) (Table 3). We did not compare the total number of NC-derived cells in the midcolon as many of the *Sox10*$^{Dom/+}$ are clearly hypoganglionic in this region.

Correlation between Disease Severity and Neuron or Glia Proportions in the Colon of the Sox10$^{Dom/+}$ Hirschsprung Disease Mouse Model

In both in vitro and in peripheral nervous structures outside the ENS, timing and levels of *Sox10* expression affect neuronal and glial fate acquisition from NC progenitors.[10–12,27,28] However, the role of *Sox10* in neuronal and glial fate acquisition in the ENS in vivo has not been determined. Feasibly, disruption of *Sox10* could alter the ratio of these cell types and contribute to GI dysfunction by impacting motility or by contributing to inflammation

Table 3. Comparison of Total NC Derivatives Between *Sox10*$^{+/+}$ and *Sox10*$^{Dom/+}$

Genotype	Region	Average NC derivatives/*mm*^{2}	SEM	*P* value
Sox10$^{+/+}$	Duodenum	3155	±57	.86
Sox10$^{Dom/+}$	Duodenum	3194	±41	
Sox10$^{+/+}$	Ileum	4555	±26	.55
Sox10$^{Dom/+}$	Ileum	4384	±44	

NOTE: Total NC derivatives per mm^2 are comparable in the duodenum and ileum of *Sox10*$^{+/+}$ and *Sox10*$^{Dom/+}$ pups. (n = 5 per genotype) No comparisons with the midcolon were made because many *Sox10*$^{Dom/+}$ mice are hypoganglionic in this region.

secondary to perturbing enteric glia.[29] To examine the possibility that ratios of enteric neurons and glia are abnormal in *Sox10*$^{Dom/+}$ pups, we quantified the proportions of neurons and glia out of total NC derivatives within the myenteric plexus at P15–17. Because different regions of the bowel have distinct functions and it is unknown how proximal to regions of aganglionosis aberrancies in lineage segregation might occur, we assessed neuron and glia proportions in the duodenum, ileum, and midcolon. Enteric neurons (Hu+)[20] and glia (FoxD3+)[29] (Figure 2) were IHC labeled, counted, and their proportions out of the total NC derivatives calculated (Figure 3*A*). Proportions of neurons and glia were found to be comparable within the duodenum (neurons $P = .28$; glia $P = .36$) and the ileum (neuron $P = .78$; glia $P = .50$) between *Sox10*$^{Dom/+}$ and *Sox10*$^{+/+}$ animals (Figure 3*B* and *C*).

Although neuronal and glial proportions in the midcolon revealed no statistically significant difference between *Sox10*$^{Dom/+}$ and *Sox10*$^{+/+}$ animals (neurons $P = .06$; glia $P = .37$), we noted an overall decrease in neuron proportions and an overall increase in glia proportions in *Sox10*$^{Dom/+}$ mice (Figure 3*B* and *C*).

Given the variable length of aganglionosis present in HSCR *Sox10*$^{Dom/+}$ mice, which models that seen in HSCR patients,[4,26] we compared colonic neuronal and glial proportions against the length of colonic aganglionosis for each *Sox10*$^{Dom/+}$ mouse. This analysis detected a strong inverse correlation between neuron proportions and length of colonic aganglionosis ($^*P < .003$; $r^2 = 0.70$) (Figure 3*D*). Conversely, a strong direct relationship is present between glia proportions and extent of colonic aganglionosis ($^*P < .005$; $r^2 = 0.66$) (Figure 3*D*). Thus, although neuron and glia proportions in the *Sox10*$^{Dom/+}$ small intestine are not altered and do not correlate with aganglionosis; in the colon, neuronal numbers decrease in concert with an increase in glial numbers as the area of the bowel affected by aganglionosis increases. Correlation scores for cell type proportions and extent of aganglionosis for each region of the bowel examined are summarized in Table 4.

Rare, Enteric Neural Crest-Derived Cell Types in Sox10$^{+/+}$ *and* Sox10$^{Dom/+}$ *Mice*

Given the presence of multiple lineages, including myofibroblasts, in colonies grown from cultured enteric NCPs in vitro,[11,12,30,31] we anticipated the possibility of identifying cells within the ENS that express neither neuronal nor glial markers. Use of the *Sox10*-Cre transgene system revealed enteric NC derivatives that were not labeled by neuronal (Hu+) or glial (FoxD3+) immunoreagents. However, these cells were extremely rare within myenteric ganglia and primary connectives with an average incidence of 1.5 cells in 1000 NC derivatives in the duodenum, 0.6 cells in 1000 in the ileum, and 6 cells in 1000 in the colon. The presence of this cell type did not statistically significantly differ between *Sox10*$^{+/+}$ and *Sox10*$^{Dom/+}$ in any region of the intestine tested (duodenum $P = .41$; ileum $P = .90$; colon $P = .23$) (Figure 4*A*). Furthermore, the proportions of this cell type did not correlate with the length of aganglionosis (Table 4).

Concurrently, while evaluating neuron and glia proportions, we documented a relatively infrequent population of enteric NC-derived cells that expressed both neuronal (Hu+) and glial (FoxD3+) markers. These cells were typically found in small clusters—mainly as couplets, triplets, or quadruplets—but occasionally found singularly (Figure 4*B*). This cell type was very rare in both *Sox10*$^{+/+}$ and *Sox10*$^{Dom/+}$ mice, and its rate of appearance did not differ between *Sox10*$^{+/+}$ and *Sox10*$^{Dom/+}$ mice in the duodenum ($P = .71$) or ileum ($P = .12$). Although they were still rare, *Sox10*$^{Dom/+}$ mice had more of these double-positive cells within the colon

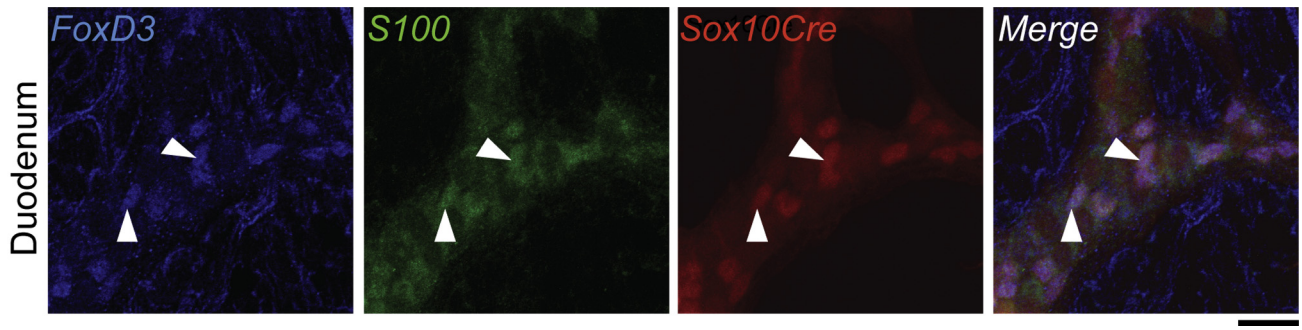

Figure 2. FoxD3 expression overlaps with S100, a known glial marker in the ENS, and readily identifies enteric glia that derive from NCPs permanently labeled by *Sox10*-Cre action on *R26R*^{tdTom} in the wild-type duodenum (*arrowheads*) (n = 3). *Scale bar* = 20 μm.

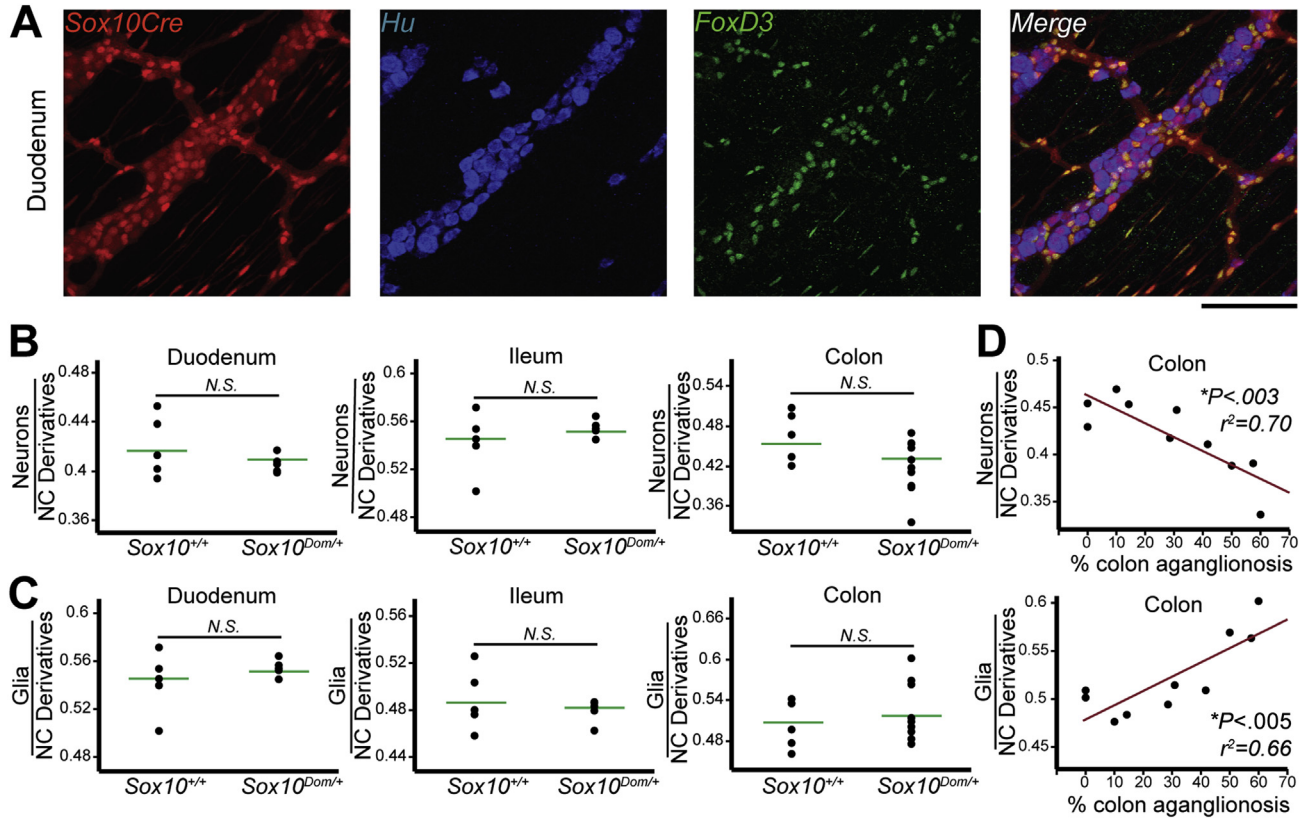

Figure 3. Proportions of neurons and glia in the colon correlate with length of aganglionosis in *Sox10*$^{Dom/+}$ mice. The proportion of enteric neurons and glia relative to the total number of NC derivatives labeled by the recombined *R26R*^{tdTom} was quantified by immunofluorescent labeling of neurons (Hu+) and glia (FoxD3+). (*A*) Representative image of *Sox10*$^{+/+}$ duodenum IHC. Scale bar = 100 μm. (*B*) The mean proportion of neurons (Hu+) was comparable between *Sox10*$^{+/+}$ and *Sox10*$^{Dom/+}$ mice in the duodenum ($P = .28$) and ileum ($P = .78$), but decreased in the colon ($P = .063$) (n = 5 per genotype). (*C*) The mean proportion of glia (FoxD3+) was comparable between *Sox10*$^{+/+}$ and *Sox10*$^{Dom/+}$ mice in the duodenum ($P = .36$), ileum ($P = .50$), and colon ($P = .37$). (*D*) Plots of neuron and glia proportions relative to length of colon aganglionosis. The proportion of NC derivatives that are neurons (Hu+) decreases as the length of colon affected by aganglionosis increases (*$P < .003$; $r^2 = 0.70$). Conversely, the proportion of glia (FoxD3+) increases as the severity of the disease increases (*$P < .005$; $r^2 = 0.66$; n = 10). N.S. = not statistically significant. *Statistically significant *P* values.

(*$P < .005$). On average, *Sox10*$^{Dom/+}$ colon samples contained 40 Hu+FoxD3+ cells per 1000 NC derivatives whereas *Sox10*$^{+/+}$ colons only contained 25 Hu+FoxD3+ cells per 1000 NC derivatives. Unlike neurons and glia, the proportion of this cell type did not correlate with disease severity in the colon of *Sox10*$^{Dom/+}$ mice ($P = .80$; $r^2 = 0.01$). Additionally, no correlations were identified for this cell type in regions of the small intestine (Table 4).

Table 4. Correlation Scores for NC-Derived Cell Types and Length of Aganglionosis in the Duodenum, Ileum, and Colon of *Sox10*$^{Dom/+}$ Pups

	Duodenum		Ileum		Colon	
Cell type	r^2	*P* value	r^2	*P* value	r^2	*P* value
Neurons (all)	0.43	.23	0.29	.35	0.70	<.003[a]
Glia	0.43	.23	0.12	.57	0.66	<.005[a]
Hu+FoxD3+ NC derivatives	0.01	.91	0.22	.43	0.01	.80
Hu-FoxD3− NC derivatives	0.07	.66	0.07	.66	0.07	.46
Calretinin+ neurons	0.09	.56	0.11	.51	0.84	<.0001[a]
nNOS+ neurons	0.07	.68	0.18	.48	0.74	<.0014[a]

[a]Statistical significance.

Regional Alterations among Enteric Neuronal Subtypes in Sox10$^{Dom/+}$ *Mice*

Because clinicians have identified chronic constipation and incontinence as problematic long-term outcomes in Hirschsprung patients,[7] we examined the relative proportions of two resident neuronal subtypes in *Sox10*$^{Dom/+}$ mutants with well-known roles in GI motility. Calretinin is expressed in cholinergic neurons, and its presence identifies excitatory muscle motor neurons within the myenteric plexus as well as some interneurons and intrinsic primary afferent neurons.[1,32] Therefore, alterations in calretinin-expressing (calretinin+) neuron numbers could affect intestinal contraction dynamics and overall motility. The proportion of calretinin+ neurons out of total neurons (Hu+) in the myenteric plexus was quantified through IHC

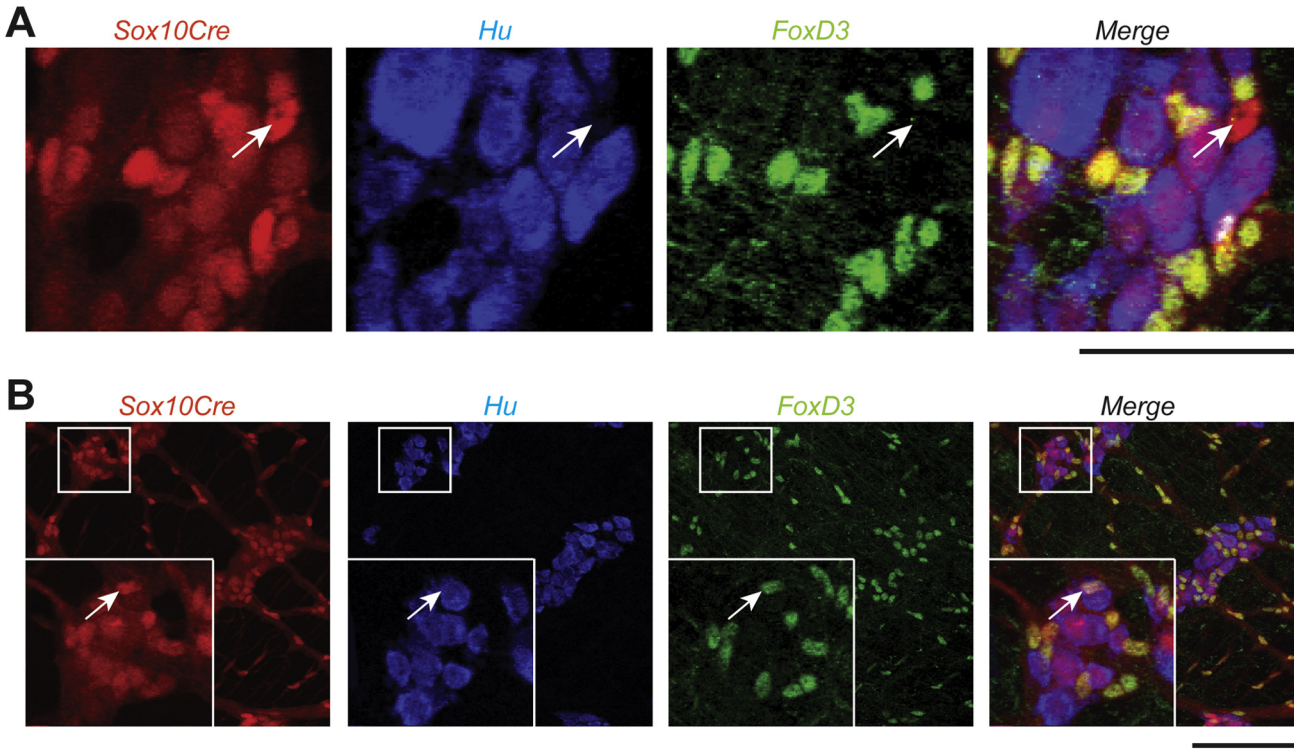

Figure 4. Rare NC derivatives in the ENS. (*A*) In this representative image of the duodenum in a $Sox10^{+/+}$ mouse, all neural crest derivatives are labeled by *Sox10*-Cre transgene driven expression of the $R26R^{tdTom}$ reporter. Immunohistochemistry was used to label neurons (Hu+) and glia (FoxD3+). The arrow denotes a NC-derived cell that does not immunohistochemically label with a neuronal (Hu+) or glial (FoxD3+) marker. These cells were extremely rare in both $Sox10^{+/+}$ and $Sox10^{Dom/+}$ mice, and the proportion of this cell type to total NC derivatives did not differ between the two phenotypes in any region of the intestine (duodenum, $P = .41$; ileum, $P = .90$; colon, $P = .23$). (*B*) The arrow in the inset denotes NC-derived cells that label with both a neuronal (Hu+) and glial (FoxD3+) marker. These cells were sometimes found alone, but many times are found in groups, such as couplets (n = 5 per genotype). *Scale bar* = 100 μm.

analysis (Figure 5*A*). The proportion of calretinin+ neurons in $Sox10^{Dom/+}$ mice duodenum was statistically significantly greater compared with $Sox10^{+/+}$ littermates ($^*P < .05$) (Figure 5*B*). Calretinin+ neurons were also present in higher proportions in the ileum of $Sox10^{Dom/+}$ mice ($^*P < .03$) (Figure 5*C*). In sharp contrast to the findings in the small intestine, an overall decrease in the proportion of calretinin+ neurons was evident in the colon. ($^*P < .03$) (Figure 5*D*). Concurrently, greater variance in colonic calretinin+ neuronal subtype proportions was present in $Sox10^{Dom/+}$ mutants compared with $Sox10^{+/+}$ samples, similar to the effect seen for colonic neuronal and glial proportions.

We tested the relationship between calretinin+ neuron proportions and length of aganglionosis. This analysis revealed that calretinin+ neuron proportions decrease dramatically as the length of aganglionosis increases ($^*P < .0001$, $r^2 = 0.84$) (Figure 5*E*). This effect was limited to the colon as calretinin+ neuron proportions did not correlate with length of aganglionosis in the duodenum nor ileum (Table 4).

To further define alterations in other motor neuron types, we evaluated neuronal nitric oxide synthase (nNOS)-expressing neurons in $Sox10^{Dom/+}$ mutants (Figure 6*A*). Nitrergic (nNOS+) neurons in the myenteric plexus are primarily inhibitory motor neurons responsible for the relaxation of intestinal smooth muscle and also include some interneurons.[1] Interestingly, although calretinin+ neuron proportions were altered in the duodenum in $Sox10^{Dom/+}$ mice, nNOS+ neuron proportions were comparable between $Sox10^{+/+}$ and $Sox10^{Dom/+}$ animals ($P = .68$) (Figure 6*B*). Similarly, nNOS+ proportions were nearly identical in the ileum between the two genotypes ($P = .51$) (Figure 6*C*). However, there was a trending increase in nNOS+ neuron proportions in the colon of $Sox10^{Dom/+}$ mice compared with $Sox10^{+/+}$ controls ($P = .099$) (Figure 6*D*).

While calretinin+ neuron proportions in the colon decreased as length of aganglionosis increased, the opposite was true for nNOS+ neurons. Animals with a greater extent of aganglionosis also exhibited a greater proportion of colonic nNOS+ neurons ($^*P = .0014$, $r^2 = 0.74$) (Figure 6*E*). Like the majority of cell types we evaluated, correlations for nNOS+ neurons were only detected in the colon and not the duodenum and ileum (Table 4).

Gastric Emptying and Small Intestinal Transit in $Sox10^{Dom/+}$ *Hirschsprung Disease Mice*

Substantial numbers of HSCR patients suffer GI dysfunction even after surgical resection of aganglionic regions. Given the skewing of neuron proportions observed in

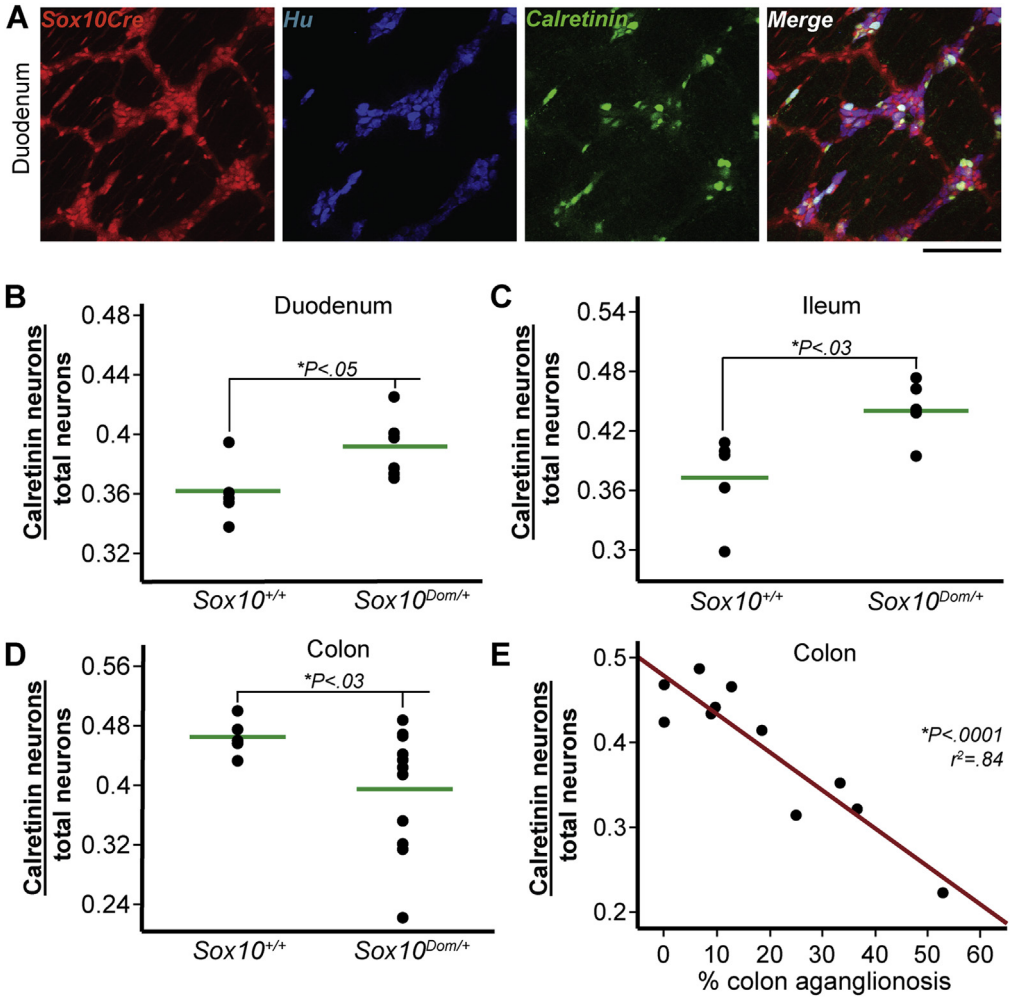

Figure 5. In *Sox10*$^{Dom/+}$ mice, calretinin neuron proportions are more abundant in the duodenum and ileum, but decreased in the colon. (*A*) Colocalization of *R26R*^{tdTom} reporter-labeled enteric NC with total neurons (Hu+) and calretinin-expressing neurons (calretinin+) allows quantitation of calretinin+ neuron proportions, as illustrated in representative images of *Sox10*$^{+/+}$ duodenum. *Scale bar* = 100 μm. *Sox10*$^{Dom/+}$ mice have an increase in calretinin+ neurons in the (*B*) duodenum (*$P < .05$) and (*C*) ileum (*$P < .03$), but exhibit a decrease in the (*D*) colon (*$P < .03$) (n = 5–6 per genotype). (*E*) Plot of calretinin+ neuron proportion versus length of aganglionic colon segment reveals a sharp decrease in calretinin+ neurons as disease severity increases. (*$P < .0001$; $r^2 = 0.84$; n = 11.)

Sox10$^{Dom/+}$ animals resulting from increased calretinin+ neurons in the duodenum and ileum, we examined GI motility dynamics proximal to the colon in *Sox10*$^{Dom/+}$ mice. To evaluate gastric emptying and small intestine transit rates, we gavaged fasted mice with a nonabsorbable fluorescent meal. Gastric emptying was determined by calculating the proportion of fluorescent signal that had left the stomach to the total recovered fluorescence, and small intestine transit rates were determined by calculating the geometric mean of fluorescence within the small intestine.[18–20] Because distal intestinal obstruction and colonic distension can affect GI transit more proximally and pups with severe aganglionosis often succumb to megacolon around weaning, we chose to limit our analysis to more mature *Sox10*$^{Dom/+}$ mice that survived past weaning to 4 weeks or 6 weeks of age. The *Sox10*$^{Dom/+}$ animals that survive to adulthood typically have a short length of aganglionosis, reach their full adult size, and feed and breed normally.

Initially, gastric emptying and small intestine transit rates were compared in 4-week-old *Sox10*$^{Dom/+}$ and *Sox10*$^{+/+}$ animals. Because HSCR shows a sex bias in humans, with three in four HSCR patients being male,[2] we evaluated GI motility in both *Sox10*$^{Dom/+}$ male and female mice. In 4-week-old animals, *Sox10*$^{Dom/+}$ males had a statistically significantly slower small intestinal transit rate compared with *Sox10*$^{+/+}$ males (*$P < .04$) (Figure 7*A*). Nearly identical results were obtained for females, with 4-week-old *Sox10*$^{Dom/+}$ females also showing statistically significantly reduced small intestinal transit rates (*$P < .006$) (Figure 7*B*). The gastric emptying rates were comparable between *Sox10*$^{Dom/+}$ and Sox10$^{+/+}$ mice for both sexes at this age (males: $P = .96$; females: $P = .68$) (Figure 7*A* and *B*).

These findings are not surprising given the skew of neuronal subtypes we observed in the small intestine of *Sox10*$^{Dom/+}$ and the known outcomes among HSCR patients. However, because neurally mediated traits are susceptible to change upon increased exposure to sex hormones,[33,34] gastric emptying and small intestine transit rates were also evaluated in older, sexually mature (6-week+) animals. For older male mice, we observed statistically comparable small intestine transit rates between *Sox10*$^{Dom/+}$ males and their wild-type *Sox10*$^{+/+}$ counterparts ($P = .57$). But, in contrast to the phenotype of 4-week-old males, we observed a marked increase in gastric emptying rates of 6-week-old *Sox10*$^{Dom/+}$ males that was not observed in 6-week-old

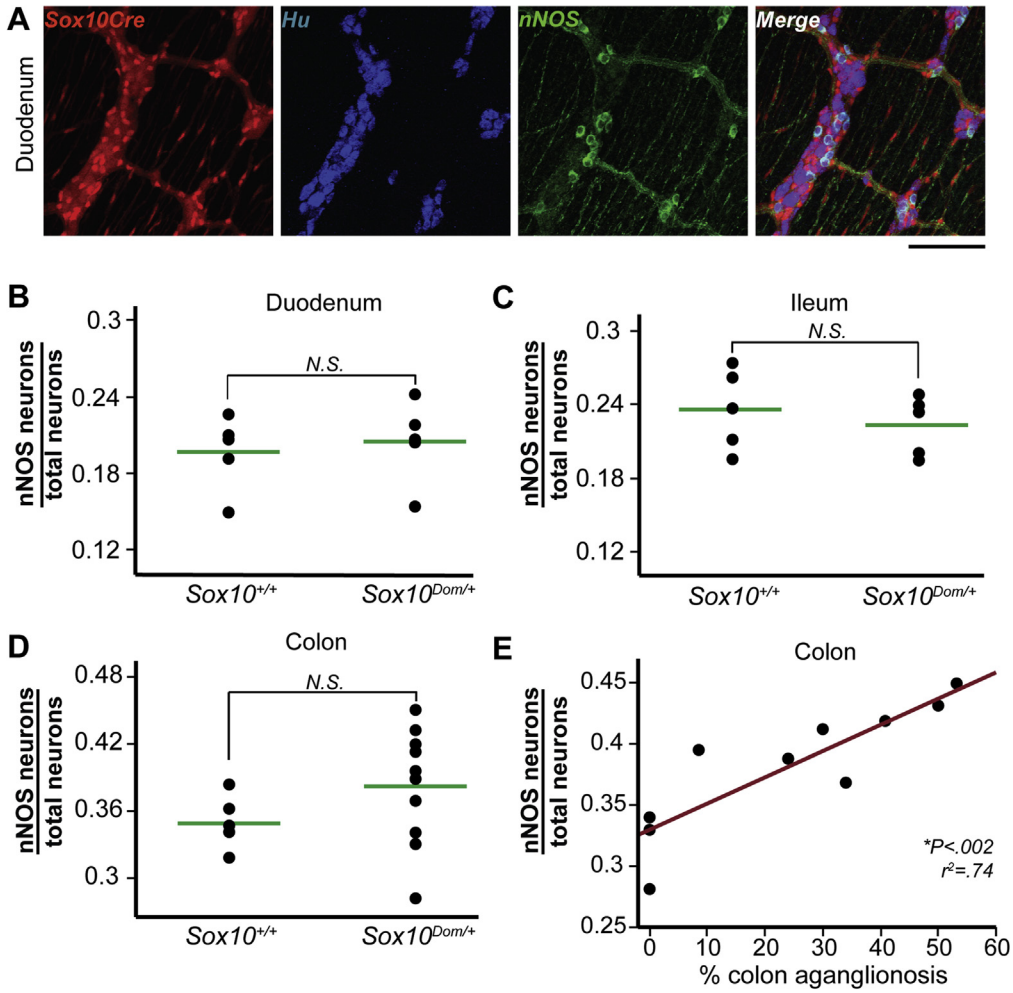

Figure 6. nNOS+ neuron proportions are comparable in *Sox10*$^{Dom/+}$ and *Sox10*$^{+/+}$ duodenum and ileum, although the proportion of nNOS+ neurons in the colon increases with aganglionosis length in the *Sox10*$^{Dom/+}$ colon. (*A*) Colabeling by the *Sox10*-Cre transgene system and nNOS IHC to quantify nNOS+ neuron proportions is shown in a *Sox10*$^{+/+}$ duodenum. *Scale bar* = 100 μm. Comparison of nNOS+ neuron proportions in the (*B*) duodenum (P = .68), (*C*) ileum (P = .51), and (*D*) colon (P = .099). (n = 5 per genotype). (*E*) Plot of nNOS+ neurons versus length of aganglionic colon segment reveals an increase in nNOS+ neuron proportion as the length of colonic aganglionosis increases. (*P < .002; r^2 = 0.74; n = 10.)

normal *Sox10*$^{+/+}$ littermates (*P < .005) (Figure 7*C*). Small intestine transit rates were comparable between 6-week-old *Sox10*$^{Dom/+}$ and *Sox10*$^{+/+}$ females (P = .31) (Figure 7*D*). And, unlike the 6-week-old males, female 6-week-old *Sox10*$^{Dom/+}$ and *Sox10*$^{+/+}$ mice had comparable gastric emptying rates (P = .58) (Figure 7*D*). To summarize, at an early age, both female and male *Sox10*$^{Dom/+}$ mice have significant small intestine transit deficits; however, in older *Sox10*$^{Dom/+}$ animals, only males exhibit any type of motility defect. (See Table 5 for a numerical summary of GI transit results.)

Sox10$^{Dom/+}$ *Mice Exhibit Negligible Colonic Inflammation*

Many Hirschsprung patients suffer from severe bouts of enterocolitis, and previous studies reported that some animals with an *Ednrb* HSCR mutation suffer from enterocolitis that can ultimately lead to bowel perforation, sepsis, and death.[22,35] Additionally, inflammatory processes within the bowel could potentially affect GI motility, making it difficult to determine whether GI motility deficits in *Sox10*$^{Dom/+}$ mice result from changes in electrical properties due to ENS deficits and/or influences of inflammatory processes on the bowel.

To determine whether enterocolitis could be affecting GI motility in adult *Sox10*$^{Dom/+}$ mice, we harvested entire colons from *Sox10*$^{Dom/+}$ and *Sox10*$^{+/+}$ 6-week+ littermates. Colons were stained with H&E and scored for inflammation by a pathologist blinded to genotype. We adopted a grading rubric for inflammation based on previous studies in HSCR mouse mutants.[22] Briefly, each mouse was assigned an inflammation score (0–7) based on the severity (0–3) and depth (0–4) of inflammation. Interestingly, *Sox10*$^{Dom/+}$ mice had no or very little inflammation, comparable to their wild-type littermates (P = .99) (Figure 8*A* and *B*).

Because males and females may differ in the levels of inflammation, we also compared inflammation scores by sex. Even when separated by sex, we observed similar levels of inflammation in *Sox10*$^{Dom/+}$ and *Sox10*$^{+/+}$ mice (Figure 8*C* and *D*). Other hallmark features of Hirschsprung disease as reported in HSCR patients, such as regions of hypoganglionosis proximal to aganglionosis and thickened muscularis propria, were evident (Figure 8*A*). Given the intestinal transit alterations in *Sox10*$^{Dom/+}$ and the lack of inflammation in this HSCR model, our results

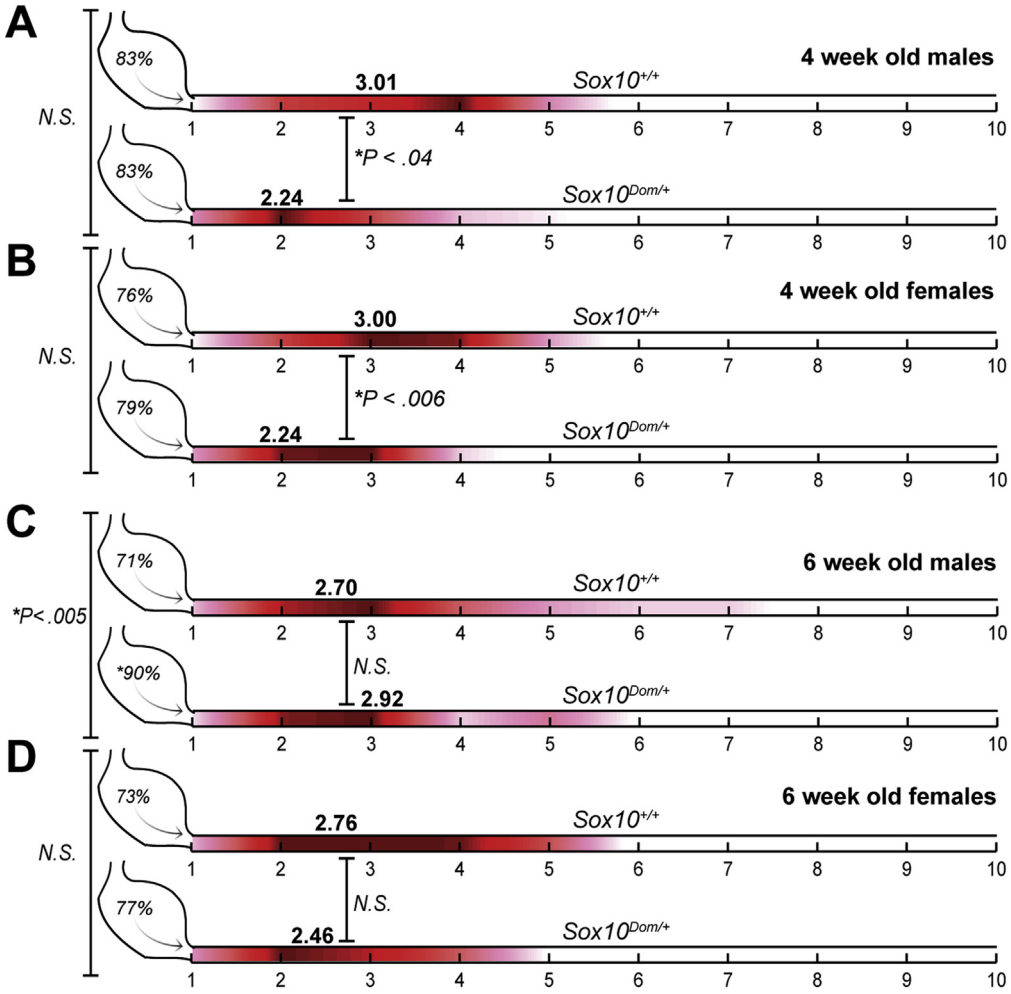

Figure 7. Comparison of gastric emptying and small intestinal transit in *Sox10*$^{+/+}$ and *Sox10*$^{Dom/+}$ mice. Schematic illustrating gastric emptying (stomach %) and small intestine transit score (red heat map) in 4-week-old and 6-week-old *Sox10*$^{+/+}$ and *Sox10*$^{Dom/+}$ males and females (n = 6–8 mice per genotype, gender, and age). The red heat map was generated by calculating the average contribution (amount of fluorescent signal) to the small intestine transit score; hotter colors (*red*) indicate a high contribution while cool colors (*pink*) indicate little contribution to the score. Average transit scores (geometric mean of fluorescence) are included in bold lettering above small intestine renditions for each group. Four-week-old *Sox10*$^{+/+}$ and *Sox10*$^{Dom/+}$ (*A*) males and (*B*) females have comparable gastric emptying, but both *Sox10*$^{Dom/+}$ sexes show slower intestine transit rates. (*C*) Six-week-old *Sox10*$^{Dom/+}$ males have faster gastric emptying but comparable small intestine transit rates to *Sox10*$^{+/+}$ males. (*D*) Six-week-old female genotypes were comparable for both gastric emptying and small intestine transit. (See *Methods* for details regarding transit scoring.)

Table 5. Comparison of Gastric Emptying and Small Intestine Transit Scores between *Sox10*$^{+/+}$ and *Sox10*$^{Dom/+}$ Mice

	Characteristics		Gastric emptying		Small intestine motility	
Genotype	Age (*wk*)	Sex	Percentage	*P* value	Percentage	*P* value
Sox10$^{+/+}$	4	M	83.09 ± 2.68	.96	3.01 ± 0.23	.04[a]
Sox10$^{Dom/+}$	4	M	83.40 ± 5.31		2.24 ± 0.21	
Sox10$^{+/+}$	4	F	76.44 ± 4.05	.68	3.00 ± 0.19	<.006[a]
Sox10$^{Dom/+}$	4	F	78.78 ± 3.74		2.24 ± 0.08	
Sox10$^{+/+}$	6	M	70.91 ± 4.16	<.005[a]	2.70 ± 0.24	.57
Sox10$^{Dom/+}$	6	M	89.50 ± 2.14		2.92 ± 0.29	
Sox10$^{+/+}$	6	F	72.94 ± 5.56	.31	2.76 ± 0.20	.58
Sox10$^{Dom/+}$	6	F	77.11 ± 4.69		2.46 ± 0.20	

NOTE: n = 6–8 mice per genotype, gender, and age.
[a]Statistical significance.

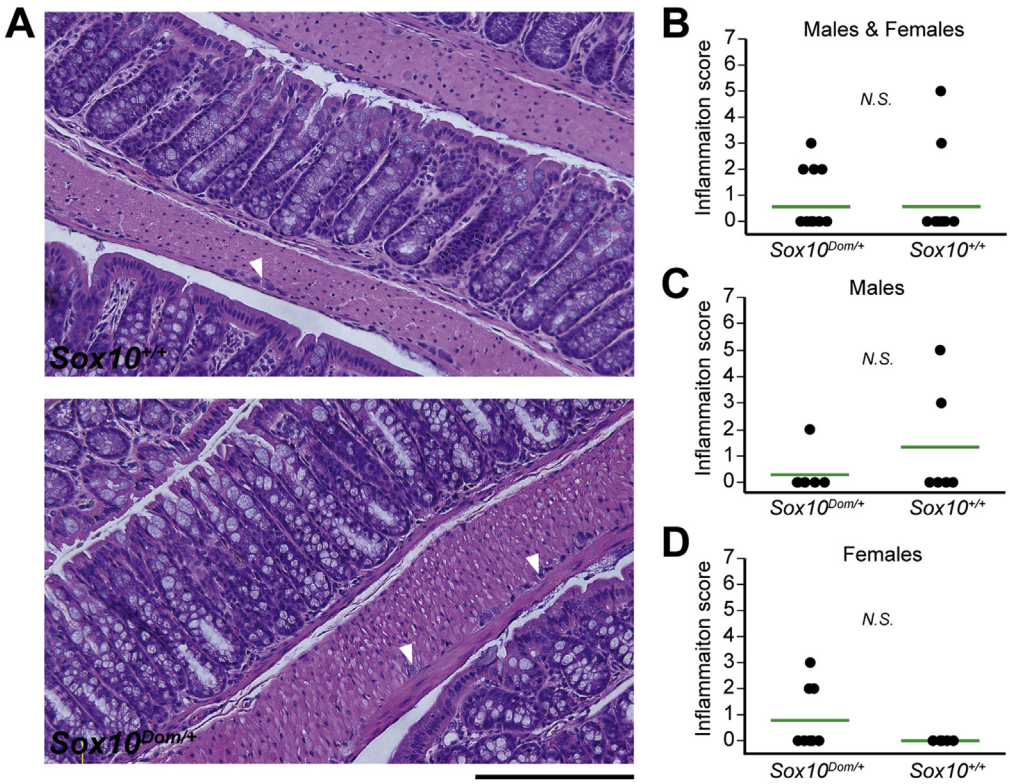

Figure 8. Comparison of inflammation in *Sox10*$^{+/+}$ and *Sox10*$^{Dom/+}$ mice. (*A*) H&E stained sections of colon in *Sox10*$^{+/+}$ (*upper panel*) and *Sox10*$^{Dom/+}$ (*lower panel*) mice demonstrate no or very little inflammation. However, note the thickened muscle and small ganglia (*arrowhead*) denoting hypoganglionosis in the *Sox10*$^{Dom/+}$ image, a common finding in Hirschsprung disease. *Scale bar* = 200 μm. (*B*) Comparison of inflammation scores (range: 0–7) between genotypes reveals no statistically significant difference in inflammation levels ($P = .99$). [*Sox10*$^{Dom/+}$ = 0.56 ± 1.03 (n = 16); *Sox10*$^{+/+}$ = 0.57 ± 1.50 (n = 14).] (*C*) Comparison of males alone yielded comparable scores between the two genotypes ($P = .30$). [*Sox10*$^{Dom/+}$ = 0.29 ± 0.76 (n = 7); *Sox10*$^{+/+}$ = 1.33 ± 2.16 (n = 6).] (*D*) Comparison of females alone also yielded comparable scores between the two genotypes ($P = .09$) [*Sox10*$^{Dom/+}$ = 0.78 ± 1.20 (n = 9); *Sox10*$^{+/+}$ = 0.00 ± 0.00 (n = 8)].

suggest the motility deficits in this HSCR model are neurally mediated.

Discussion

The *Sox10*$^{Dom/+}$ HSCR mutant is one of several HSCR models frequently studied to better understand the NC deficits that give rise to aganglionosis.[2,9,28,36] The *Sox10*^{Dom} allele disrupts migration of enteric NCPs and contributes to extensive colonic aganglionosis.[37,38] Additionally, isolated *Sox10*$^{Dom/+}$ enteric NPCs do not produce a normal profile of cell lineages when cultured in vitro.[12] Despite the insights gained from studying the fetal effects of *Sox10* mutations on NCP migration and consequent aganglionosis, no prior efforts have investigated postnatal consequences of *Sox10* mutations on ganglionated regions. In this study, we undertook a comprehensive assessment of NC derivatives in the proximal, ganglionated intestine of *Sox10*$^{Dom/+}$ mice to test the hypothesis that the *Sox10*^{Dom} mutation leads to imbalances in enteric NC-derived lineages and deficits in bowel function. Our analysis revealed effects of the *Sox10* mutation on neuronal-glial lineage segregation in the colon but not the small intestine. Interestingly, this study identified significant imbalances in proportions of excitatory and inhibitory enteric neurons accompanied by deficits in intestinal transit and gastric emptying. Calretinin+ neurons with roles in muscle contraction were significantly increased in the duodenum and ileum while nNOS+ neurons with roles in muscle relaxation were unchanged in these regions.

Sox10 effects on glial cell specification and NCP multipotency are well established in other aspects of the peripheral nervous system such as the dorsal root ganglion.[10,27,28,39] Surprisingly, our analysis indicated no effect of the *Sox10*^{Dom} mutation on neuronal-glial balance in the duodenum and ileum although there was a statistically significant correlation between the proportion of neurons and glia in the *Sox10*^{Dom} colon and the overall extent of aganglionosis. It is possible that *Sox10*$^{Dom/+}$ neurons and glia are born in equal proportions in the colon, with more neurons subsequently succumbing to apoptosis while glia persist. However, increased apoptosis has not been observed in several ENS mutants to date.[12,40,41] Moreover, cell death cannot adequately account for the observed increases in colonic nNOS+ neuron proportions to levels well above the wild-type average in *Sox10*$^{Dom/+}$ mice with severe aganglionosis. Our study suggests that the timing of NCP lineage choice is likely a key factor in determining not only

the length of aganglionosis but ultimately the proportions of enteric glia, neurons, and neuronal subtypes.

It has been postulated that premature neuronal differentiation contributes to HSCR disease by depleting the enteric NCP pool. Premature NCP differentiation would not only exhaust the NCP pool, but may cause certain cell types to be born more or less often based on when (temporally) and where (local environment) lineage choice occurs. This phenomenon could account for the region-specific imbalance of different NC-derived cell types we observed in *Sox10*$^{Dom/+}$ mice. Such a possibility is corroborated by recent findings in the developing telencephalon, where oscillating or sustained expression of specific transcription factors controls whether neural progenitor cells go on to differentiate into specific cell types or continue to proliferate and give rise to daughter neural progenitor cells.[42]

Given the diversity of cell types that can arise from cultured NC progenitors in vitro,[43] we were not surprised to identify NC-derived cells in the intestine that did not label with neuronal or glial immunoreagents. These cells are infrequent and might represent a novel cell type or possibly cell turnover within ganglia. Because proportions of these NC-derived cells were equivalent between P15–19 *Sox10*$^{Dom/+}$ and *Sox10*$^{+/+}$ animals and because they were so rare, we did not attempt to characterize this lineage further. Interestingly, in both *Sox10*$^{Dom/+}$ and *Sox10*$^{+/+}$ mice, we observed cells that double-labeled with neuronal (Hu+) and glial (FoxD3+) markers. This cell type may represent either a novel lineage or a progenitor(s) undergoing differentiation. Given their morphology and tendency to be found in clusters, these cells could also represent neural progenitors with adjacent daughter progenitors or daughter cells not fully committed to a specific cell type. The latter is certainly feasible given that FoxD3 is expressed in enteric NCPs as well as enteric glia.[29,44] Enteric neural progenitors certainly exist in the adult intestine, and their exact location and nature are being actively investigated.[21,24,31] However, no markers have been found that exclusively label neural stem cells in the intestine, convoluting efforts to characterize this cell type. If truly an enteric neural stem cell, the increase in this cell type in the *Sox10*$^{Dom/+}$ colon might represent a futile attempt by the remaining neural stem cells to populate the hypoganglionic or aganglionic areas of the distal intestine.

Because HSCR is a multigenic disorder, whereby an independent variant in any one of several genes can produce aganglionosis, our findings are potentially of broad relevance to other HSCR models. HSCR mouse models with deficiency of *Edn3* or *Ednrb* were also found by Sandgren et al (2002) and Zaitoun et al (2013), respectively, to exhibit increases in nNOS+ expressing neurons in the colons of these models.[23,45] However, NC-derived cell type proportions and their correlations with length of aganglionosis were not reported. Our analysis benefited from the varying levels of aganglionosis present with the *Sox10*$^{Dom/+}$ mutation on a mixed background, and this type of analysis may not have been possible in other HSCR mouse models where extent of aganglionosis is confined to a small region of distal colon.[46] This type of analysis is important, as similar perturbations of NC fate choice may be occurring in HSCR patients and thus the length of aganglionosis could inform patient outcomes and care in the future.

Furthermore, these other studies did not evaluate any regions of the intestine proximal to the ileum. For the first time, we report alterations in NC-derived proportions (calretinin+ neurons specifically) within the proximal small intestine (duodenum) of a HSCR mouse model. The mechanisms driving the altered proportions of NC derivates within HSCR mutants are unclear at this time. Prenatal obstruction (atresia) has been shown to affect NC derivatives in rats,[47] and the extent of aganglionosis in the *Sox10*^{Dom} HSCR model may effectively be producing a varying length of obstruction. We realize obstruction cannot be excluded as a factor that impacts NC derivative choice; however, *Sox10*$^{Dom/+}$ mice are born in Mendelian ratios relative to their wild-type littermates, and the majority survive to weaning, which suggests that obstruction does not play a large role prenatally. We specifically elected to examine P15–19 pups for NC-derived lineages to ensure that the ENS was fully developed and at the same time to try to avoid influences of obstruction on the ENS. (The majority of *Sox10*$^{Dom/+}$ mice that suffer from obstruction succumb to megacolon near or at weaning when they transition to solid food.)

Mice with deficits in ENS patterning or NCP lineage segregation can exhibit altered GI motility even when no aganglionosis is present.[9,20] However, HSCR models have not previously been evaluated for motility deficits within ganglionated regions of the small intestine. Many studies limit their analysis to male mice, but we chose to examine both males and females given the difference in incidence of HSCR and other neurodevelopmental disorders between males and females. In the *Sox10*$^{Dom/+}$ model, we documented slower small intestine transit rates in 4-week-old males and females. Because *Sox10*$^{Dom/+}$ mice show increases in excitatory motor neurons (calretinin+) in the small intestine but no changes in inhibitory motor neurons (nNOS+), we hypothesize that imbalances in motor neuron cell types cause changes in peristalsis coordination and/or neuron signaling. Because other neuronal subtypes also affect motility, we cannot at this time directly attribute these changes in GI motility to our findings in calretinin+ and nNOS+ neurons. However, given that calretinin+ and nNOS+ neurons comprise the majority of motor neurons in the myenteric plexus, our hypothesis provides a plausible and attractive explanation.

In contrast with our results in young animals, mature *Sox10*$^{Dom/+}$ and *Sox10*$^{+/+}$ mice showed comparable small intestine transit rates. It could be that the *Sox10*$^{Dom/+}$ intestine adapts or compensates for deficits as the ENS matures or that we have selected for more mildly affected mice at this age, as many severely affected animals succumb to HSCR megacolon near weaning. However, we also observed increased gastric emptying in older *Sox10*$^{Dom/+}$ males that we did not see in females, a result that was unexpected. Increased gastric emptying in HSCR mouse models has not previously been reported, and the underlying physiologic

basis for this effect in males is not clear. For many neurodevelopment diseases, females are postulated to be protected or differentially affected due to circulating sex hormones while males are more susceptible.[33,34] This tendency for males to be more severely affected by neurodevelopmental disorders may explain why males are afflicted more often with HSCR than females (3:1) and could explain why 6-week-old *Sox10*$^{Dom/+}$ males have increased gastric emptying rates, but not females. Furthermore, increased gastric emptying rates may confound small intestine transit rates because gastric contents are more rapidly entering the small intestine. Therefore, it is possible that our *Sox10*$^{Dom/+}$ males still have a decreased small intestine transit rate compared with their wild-type counterparts but this phenotype is being masked by increased gastric emptying.

Our analysis is the first report of altered gastric emptying and small intestine transit in a HSCR mouse model. Not surprisingly, given the presence of distal bowel aganglionosis, prior studies have reported altered or absent colonic migratory complexes in *Gdnf*, *Edn3*, and *Ednrb* HSCR mutants.[23,45,48,49] Additionally, while most studies limit their analysis to male mice, our studies identified novel deficits in gastric emptying as well as small intestine transit for the *Sox10*$^{Dom/+}$ HSCR mouse model that are age and sex dependent. Whether alterations in gastric emptying or small intestine transit are present among other HSCR mutant alleles remains to be seen. Future analyses are required to determine the exact electrophysiologic changes within the ENS in *Sox10*$^{Dom/+}$ mice and other HSCR mutants and to ascertain whether other cell types that contribute to motor activity (such as serotonergic neurons or interstitial cells of Cajal) are perturbed. Similarities and disparities in outcomes between HSCR mutant models should help elucidate exactly when and where HSCR genes act within HSCR gene pathways.

Despite the fact that infection and inflammatory processes are known to affect GI transit speed,[50] we saw no difference in colonic inflammation between *Sox10*$^{Dom/+}$ and *Sox10*$^{+/+}$ adult mice. This finding further suggests that the differences in gastric emptying and small intestine transit are most likely driven by neural mechanisms. It remains to be seen whether *Sox10*$^{Dom/+}$ mice are more or less susceptible to inflammation when challenged by surgery, infection, or chemical treatment. Some HSCR patients and mouse models are susceptible to enterocolitis, but the mechanisms driving this susceptibility are still not well understood.[7,22,35]

Collectively, this study demonstrates for the first time skewed enteric NC derivative proportions and altered GI motility in the small intestine of a HSCR mouse model. These findings demonstrate a role for *Sox10* in NC lineage specification in vivo in the ENS. Moreover, our results suggest a novel role for *Sox10* in neuronal subtype choice and demonstrate that perturbations in *Sox10* can affect GI transit in ganglionated regions of the intestine. Different regions of the *Sox10*$^{Dom/+}$ intestine were found to have distinct abnormalities, and GI transit assays revealed sex- and age-dependent effects, suggesting that timing and environment play a key role in not only NC lineage segregation but ultimately functional outcomes.

References

1. Furness JB. The enteric nervous system. Malden, MA: Blackwell, 2006.
2. Chakravarti A, Lyonett S. Hirschsprung disease. In: Scriver CR, Beaudet AL, Sly WS et al., eds. The metabolic and molecular bases of inherited disease. 8th ed. The online metabolic and molecular bases of inherited disease. New York: McGraw-Hill Global Education, 2001:6231–6255.
3. Cantrell VA, Owens SE, Chandler RL, et al. Interactions between Sox10 and EdnrB modulate penetrance and severity of aganglionosis in the *Sox10*^{Dom} mouse model of Hirschsprung disease. Hum Mol Genet 2004; 13:2289–2301.
4. Owens SE, Broman KW, Wiltshire T, et al. Genome-wide linkage identifies novel modifier loci of aganglionosis in the *Sox10*^{Dom} model of Hirschsprung disease. Hum Mol Genet 2005;14:1549–1558.
5. Alves MM, Sribudiani Y, Brouwer RW, et al. Contribution of rare and common variants determine complex diseases—Hirschsprung disease as a model. Dev Biol 2013;382:320–329.
6. Jiang Q, Ho YY, Hao L, et al. Copy number variants in candidate genes are genetic modifiers of Hirschsprung disease. PLoS One 2011;6:e21219.
7. Rintala RJ, Pakarinen MP. Long-term outcomes of Hirschsprung's disease. Semin Pediatr Surg 2012; 21:336–343.
8. Demehri FR, Halaweish IF, Coran AG, et al. Hirschsprung-associated enterocolitis: pathogenesis, treatment and prevention. Pediatr Surg Int 2013;29:873–881.
9. Musser MA, Michelle Southard-Smith E. Balancing on the crest—evidence for disruption of the enteric ganglia via inappropriate lineage segregation and consequences for gastrointestinal function. Dev Biol 2013;382:356–364.
10. Paratore C, Goerich DE, Suter U, et al. Survival and glial fate acquisition of neural crest cells are regulated by an interplay between the transcription factor Sox10 and extrinsic combinatorial signaling. Development 2001; 128:3949–3961.
11. Paratore C, Eichenberger C, Suter U, et al. Sox10 haploinsufficiency affects maintenance of progenitor cells in a mouse model of Hirschsprung disease. Hum Mol Genet 2002;11:3075–3085.
12. Walters LC, Cantrell VA, Weller KP, et al. Genetic background impacts developmental potential of enteric neural crest-derived progenitors in the *Sox10*^{Dom} model of Hirschsprung disease. Hum Mol Genet 2010;19: 4353–4372.
13. Corpening JC, Deal KK, Cantrell VA, et al. Isolation and live imaging of enteric progenitors based on *Sox10-Histone2BVenus* transgene expression. Genesis 2011; 49:599–618.
14. Postic C, Shiota M, Niswender KD, et al. Dual roles for glucokinase in glucose homeostasis as determined by liver and pancreatic beta cell-specific gene knock-outs using Cre recombinase. J Biol Chem 1999;274:305–315.

15. Crabtree JS, Scacheri PC, Ward JM, et al. Of mice and MEN1: insulinomas in a conditional mouse knockout. Mol Cell Biol 2003;23:6075–6085.
16. Boyle S, Misfeldt A, Chandler KJ, et al. Fate mapping using Cited1-CreERT2 mice demonstrates that the cap mesenchyme contains self-renewing progenitor cells and gives rise exclusively to nephronic epithelia. Dev Biol 2008;313:234–245.
17. Deal KK, Cantrell VA, Chandler RL, et al. Distant regulatory elements in a *Sox10*-beta GEO BAC transgene are required for expression of *Sox10* in the enteric nervous system and other neural crest-derived tissues. Dev Dyn 2006;235:1413–1432.
18. Miller MS, Galligan JJ, Burks TF. Accurate measurement of intestinal transit in the rat. J Pharmacol Methods 1981; 6:211–217.
19. Brun P, Giron MC, Qesari M, et al. Toll-like receptor 2 regulates intestinal inflammation by controlling integrity of the enteric nervous system. Gastroenterology 2013; 145:1323–1333.
20. D'Autreaux F, Margolis KG, Roberts J, et al. Expression level of Hand2 affects specification of enteric neurons and gastrointestinal function in mice. Gastroenterology 2011;141:576–587, e1–6.
21. Liu MT, Kuan YH, Wang J, et al. 5-HT4 receptor-mediated neuroprotection and neurogenesis in the enteric nervous system of adult mice. J Neurosci 2009; 29:9683–9699.
22. Cheng Z, Dhall D, Zhao L, et al. Murine model of Hirschsprung-associated enterocolitis. I: phenotypic characterization with development of a histopathologic grading system. J Pediatr Surg 2010;45:475–482.
23. Zaitoun I, Erickson CS, Barlow AJ, et al. Altered neuronal density and neurotransmitter expression in the ganglionated region of *Ednrb* null mice: implications for Hirschsprung's disease. Neurogastroenterol Motil 2013; 25:e233–e244.
24. Laranjeira C, Sandgren K, Kessaris N, et al. Glial cells in the mouse enteric nervous system can undergo neurogenesis in response to injury. J Clin Invest 2011; 121:3412–3424.
25. Hari L, Miescher I, Shakhova O, et al. Temporal control of neural crest lineage generation by Wnt/beta-catenin signaling. Development 2012;139:2107–2117.
26. Southard-Smith EM, Angrist M, Ellison JS, et al. The Sox10(^{Dom}) mouse: modeling the genetic variation of Waardenburg-Shah (WS4) syndrome. Genome Res 1999;9:215–225.
27. Kim J, Lo L, Dormand E, et al. SOX10 maintains multipotency and inhibits neuronal differentiation of neural crest stem cells. Neuron 2003;38:17–31.
28. Bondurand N, Sham MH. The role of *SOX10* during enteric nervous system development. Dev Biol 2013; 382:330–343.
29. Mundell NA, Plank JL, LeGrone AW, et al. Enteric nervous system specific deletion of Foxd3 disrupts glial cell differentiation and activates compensatory enteric progenitors. Dev Biol 2012;363:373–387.
30. Kruger GM, Mosher JT, Bixby S, et al. Neural crest stem cells persist in the adult gut but undergo changes in self-renewal, neuronal subtype potential, and factor responsiveness. Neuron 2002;35:657–669.
31. Bixby S, Kruger GM, Mosher JT, et al. Cell-intrinsic differences between stem cells from different regions of the peripheral nervous system regulate the generation of neural diversity. Neuron 2002;35:643–656.
32. Qu ZD, Thacker M, Castelucci P, et al. Immunohistochemical analysis of neuron types in the mouse small intestine. Cell Tissue Res 2008;334:147–161.
33. Legato MJ, Bilezikian JP. Principles of gender-specific medicine. Boston: Elsevier Academic Press, 2004.
34. Gillies GE, McArthur S. Estrogen actions in the brain and the basis for differential action in men and women: a case for sex-specific medicines. Pharmacol Rev 2010;62:155–198.
35. Zhao L, Dhall D, Cheng Z, et al. Murine model of Hirschsprung-associated enterocolitis II: surgical correction of aganglionosis does not eliminate enterocolitis. J Pediatr Surg 2010;45:206–211.
36. Amiel J, Sproat-Emison E, Garcia-Barcelo M, et al. Hirschsprung disease, associated syndromes and genetics: a review. J Med Genet 2008;45:1–14.
37. Southard-Smith EM, Kos L, Pavan WJ. Sox10 mutation disrupts neural crest development in ^{Dom} Hirschsprung mouse model. Nat Genet 1998;18:60–64.
38. Kapur RP. Early death of neural crest cells is responsible for total enteric aganglionosis in *Sox10*^{Dom}/*Sox10*^{Dom} mouse embryos. Pediatr Dev Pathol 1999;2:559–569.
39. Sonnenberg-Riethmacher E, Miehe M, Stolt CC, et al. Development and degeneration of dorsal root ganglia in the absence of the HMG-domain transcription factor *Sox10*. Mech Dev 2001;109:253–265.
40. Gianino S, Grider JR, Cresswell J, et al. GDNF availability determines enteric neuron number by controlling precursor proliferation. Development 2003;130:2187–2198.
41. Uesaka T, Jain S, Yonemura S, et al. Conditional ablation of GFRα1 in postmigratory enteric neurons triggers unconventional neuronal death in the colon and causes a Hirschsprung's disease phenotype. Development 2007; 134:2171–2181.
42. Imayoshi I, Isomura A, Harima Y, et al. Oscillatory control of factors determining multipotency and fate in mouse neural progenitors. Science 2013;342:1203–1208.
43. Coelho-Aguiar JM, Le Douarin NM, Dupin E. Environmental factors unveil dormant developmental capacities in multipotent progenitors of the trunk neural crest. Dev Biol 2013;384:13–25.
44. Teng L, Mundell NA, Frist AY, et al. Requirement for Foxd3 in the maintenance of neural crest progenitors. Development 2008;135:1615–1624.
45. Sandgren K, Larsson LT, Ekblad E. Widespread changes in neurotransmitter expression and number of enteric neurons and interstitial cells of Cajal in lethal spotted mice: an explanation for persisting dysmotility after operation for Hirschsprung's disease? Dig Dis Sci 2002; 47:1049–1064.
46. Chakravarti A, McCallion A, Lyonnet S. Multisystem inborn errors of development: Hirschsprung. In: Valle DBA, Vogelstein B, Kinzler KW, et al., eds. Scriver's online metabolic and molecular bases of inherited disease. New York: McGraw Hill Education, 2006.

47. Khen-Dunlop N, Sarnacki S, Victor A, et al. Prenatal intestinal obstruction affects the myenteric plexus and causes functional bowel impairment in fetal rat experimental model of intestinal atresia. PLoS One 2013; 8:e62292.
48. Roberts RR, Bornstein JC, Bergner AJ, et al. Disturbances of colonic motility in mouse models of Hirschsprung's disease. Am J Physiol Gastrointest Liver Physiol 2008;294:G996–G1008.
49. Ro S, Hwang SJ, Muto M, et al. Anatomic modifications in the enteric nervous system of piebald mice and physiological consequences to colonic motor activity. Am J Physiol Gastrointest Liver Physiol 2006;290:G710–G718.
50. Sharkey KA, Savidge TC. Role of enteric neurotransmission in host defense and protection of the gastrointestinal tract. Auton Neurosci 2014;181C:94–106.

Received August 1, 2014. Accepted August 5, 2014.

Correspondence
Address correspondence to: E. Michelle Southard-Smith, PhD, Division of Genetic Medicine, Department of Medicine, Vanderbilt University, 2215 Garland Ave, 529 Light Hall, Nashville, Tennessee 37232–0275. e-mail: michelle.southard-smith@vanderbilt.edu; fax: (615) 343-2601.

Acknowledgments
The authors thank Dr Sam Wells and the support staff of the Cell Imaging Shared Resource (CISR) Core at Vanderbilt for advice and assistance in confocal imaging; Maureen Gannon, Trish Labosky, Elaine Ritter, Carrie Wiese, and Kate Jones for thoughtful comments on the text; Alex Schenkman for assistance generating GI transit heat maps; Michael D. Gershon and Xiang "Sam" Li for assistance establishing and implementing GI transit assays; and Jeff Smith and Joan Breyer for use and assistance with the Molecular Devices/LJL Analyst HT. The Hu, FoxD3, and S100 antibodies were kind gifts from Vanda Lennon (Mayo Clinic), Trish Labosky (NIH) and Heather Young (University of Melbourne), respectively.

Conflicts of interest
The authors disclose no conflicts.

Funding
This study was funded by the March of Dimes [Grant FY12-450], the National Institutes of Health [Grants R01 DK60047 (to E.M.S.-S.), and F30 DK096831 (to M.A.M.)], and by a VICTR award from the National Institutes of Health CTSA award [Grant UL1TR000445 (to M.A.M.)], and National Institute of General Medical Sciences [Grant T32 GM07347] to the Vanderbilt Medical-Scientist Training Program. The Cell Imaging Shared Resource (CISR) Core at Vanderbilt is supported by the National Institutes of Health National Cancer Institute [Grant CA68485], National Institute of Diabetes and Digestive and Kidney Diseases [Grants DK20593, P50-DK58404, DK59637], *Eunice Kennedy Shriver* National Institute of Child Health and Human Development [Grant HD15052], and National Eye Institute [Grant EY08126]. Work done in the CISR was supported in part by a Digestive Disease Research Center Core Scholarship funded by National Institutes of Health National Institute of Diabetes and Digestive and Kidney Diseases [Grant P50-DK058404] and by a Vanderbilt Kennedy Center Core Scholarship funded by the *Eunice Kennedy Shriver* National Institute of Child Health and Human Development [Grant P30-HD15052.]